Diagnosis and surgical management of intussusception in an axolotl (Ambystoma mexicanum)

Sabrina Vieu, Charlotte Coeuriot, Laetitia Dorso, Marion Fusellier

Diagnosis and surgical management of intussusception in an axolotl (*Ambystoma mexicanum*)

Sabrina Vieu[1*], Charlotte Coeuriot[2*], Laetitia Dorso[3, 5], Marion Fusellier[2, 4]

[1] Service des Nouveaux Animaux de Compagnie, Oniris, CHUV, 44300 Nantes, France

[2] Service d'Imagerie Médicale, Oniris, CHUV, 44300 Nantes, France

[3] Service Autopsie, Oniris, CHUV, 44300 Nantes, France

[4] Oniris, Nantes Université, Inserm, RMeS, F-44000 Nantes, France

[5] Oniris, INRAE, BIOEPAR, 44300 Nantes, France

* co-authors

Diagnosis and surgical management of intussusception in an axolotl (*Ambystoma mexicanum*)

ABSTRACT

Background: Intussusception diagnosis and surgical management in axolotl (*Ambystoma mexicanum)* is poorly documented.

Case Description: A client-owned, five-year-old, sexually intact, female axolotl was presented for hyporexia of four-week duration associated with regurgitation after feedings. Clinical examination showed lethargy, weight loss, and firm tissue at coelomic palpation. Coelomic ultrasonography was consistent with an intestinal intussusception. An exploratory coeliotomy was performed, followed by an intestinal resection and anastomosis of a thickened portion of intestinal loop. Following surgical excision of the invaginated intestinal loops, anorexia was not resolved, and the axolotl died four days later. A necropsy revealed a serofibrinous coelomitis. Histopathology confirmed the presence of an obstructive mass in the resected portion of the intestines.

Conclusion and case relevance: This report describes an intussusception diagnosis and attempted treatment in an axolotl. Ultrasonography in axolotl with non-specific gastrointestinal symptoms is recommended for evaluation of the coelomic organs.

<u>Keywords</u>: Axolotl, Amphibian, Enterectomy, Histopathology, Intussusception, Ultrasonography

Introduction

Intussusception diagnosis and management in amphibians have been poorly documented. The following databases (PubMed and CAB) were searched with the following keywords: amphibian, axolotl, enterectomy, gastrointestinal disease, intussusception, ultrasounds, and ultrasonography on [09/17/22]; three reference textbooks were consulted.[1-3] No reports of intussusception were found with these searches. This case describes an intussusception diagnosis and attempted treatment in an axolotl.

Case presentation

A 5-year-old, 88 g, sexually intact, female, leucistic axolotl (*Ambystoma mexicanum*) was presented for hyporexia of four-week duration associated with regurgitation after feedings. Weight loss and poor general condition were noticed by the owner. The animal lived with another male axolotl in a glass tank (120 × 40 × 40 cm) with a water temperature between 18 °C and 21 °C (64.4 °F to 68 °F), an external filter, and small rocks as substrate. The diet consisted of axolotl pellets (NovoLotl; JBL) supplied once or twice a week. The axolotl last produced eggs two months earlier. Clinical examination revealed lethargy, reduced muscle mass over the spine and limbs, gill atrophy, and pale oral mucous membranes. Firm tissue was palpable in the mid-coelom.

Lateral and dorsoventral radiographs of the whole body were unremarkable. Coelomic ultrasonography (L15-7io compact linear array transducer, PHILIPS Affiniti 70G, 7-15 MHz) revealed a mid-coelomic mass effect, with a multilayered appearance of the intestinal wall in longitudinal view, consistent with intussusception. On transverse view, multiple concentric rings were present, with the outer bowel segment (intussuscipiens) hypoechoic and thickened, and a normal inner bowel segment (intussusceptum). The mesenteric fat was hyperechogenic to the surrounding tissue **(Figure 1 and Video 1)**.

Surgical intervention was elected to correct the intussusception. The axolotl was sedated with butorphanol (0.2 mg/kg intramuscular [IM]; Torphasol®, Axience, Pantin, France) and alfaxalone (5 mg/kg IM; Alfaxan®, Jurox, Dublin, Ireland). Analgesia was completed with meloxicam (0.1 mg/kg IM; Metacam®, Boehringer, Lyon, France). Sedation effects were observed in less than 5 minutes after injection, and anesthesia was induced by placing the axolotl in a bath of sterile saline [0.9% NaCl] solution with alfaxalone (12.5 mg/L) oxygenated with an oxygen concentrator (100% oxygen at 0.5 L/min). The axolotl was placed in dorsal recumbency with an ultrasound Doppler probe (Parks Medical Electronics, 811-Bts Ultrasonic Doppler Flow Detector, 8.2 MHz) placed above the heart for monitoring. Branchial and transcutaneous irrigation with alfaxalone (drop-by-drop administration of 15 mg of alfaxalone diluted in saline [0.9% NaCl] solution) was performed every 3 minutes to maintain anesthesia. The skin was cleaned with povidone-iodine applied with gauze for 15 seconds. Local anesthesia was performed with a lidocaine drop on the skin (0.5 mg/kg; Laocaine®, MSD Santé Animale, Beaucouze, France). An exploratory coeliotomy was performed through a 4 cm craniocaudal skin incision by a paramedian approach with a #11 blade. The coelomic membrane was elevated and carefully incised. Exploration of the coelomic cavity revealed a severely congested and distended intestinal loop immediately aboral to the stomach, without an intestinal segment observed between these two structures. The small intestine after the pylorus was entirely intussuscepted in the ileocolic region **(Figure 2A)**. Gentle manual traction on the intussusceptum and pressure on the intussuscipiens aided in reduction. Once the intussusception was resolved, enteric vessels were grossly normal. The bowel wall did not appear ischemic. The last portion reduced of the intussusception was the cranial part of the intestinal tract located directly aboral to the pylorus, with a major thickening over 0.75 mm in length. Firm pink nodules of 1 mm were observed on the duodenal serosa **(Figure 2D)** with yellow mesenteric nodules. The rest of the intestinal tract appeared normal. Intestinal resection and anastomosis (IRA) of the thickened portion was initiated in a similar manner as in mammals. The thickened portion was raised with cotton-tipped applicators and clamped with hemostats, separating it from the remaining viscera. The blood vessels supplying the isolated segment were ligated with a 5-0 poliglecaprone monofilament absorbable suture (Monocryl 5/0®, Ethicon, Issy-les-Moulineaux, France). The mesentery was incised near the ligated vessels. After vessel ligation, the intestinal portion was removed, and a single-layer closure was used for end-to-end anastomosis (5-0 poliglecaprone). The resected loop portion was fixed in 10% buffered formalin. The coelomic cavity was rinsed with a sterile saline [0.9% NaCl] solution. The coelomic membrane was closed with a continuous suture pattern (5-0 poliglecaprone), and the skin in a horizontal mattress pattern with a 4-0 nylon monofilament non-absorbable suture (Filapeau 4/0®, Peters Surgical, Boulogne-Billancourt, France). After surgery, the axolotl was placed in a water bath with oxygen delivered by an oxygen concentrator (100% oxygen at 0.5 L/min) for recovery and was fully awake in 60 minutes.

One day after the surgery, the axolotl was discharged with metronidazole (10 mg/kg per os q24 h; Flagyl® 125 mg/mL, Sanofi Aventis, Gentilly, France) for 7 days. However, two days later, the axolotl became more lethargic, developed an abnormal position in the water column, and died four days after the surgery. No signs of appetite were observed.

At necropsy, no signs of skin or coelomic membrane dehiscence were noted. A serofibrinous coelomitis characterized by the presence of a light brown serofibrinous effusion of 2 ml and brown coloration of the entire thickness of the intestinal tract and of the parietal coelom caudally to the IRA site was observed **(Figure 3)**. The remainder of the examined tissues were unremarkable. The IRA and intestinal mesentery closure were in place.

Histological examination of the surgically resected loop revealed a multilobulated, non-encapsulated mass, protruding widely into the lumen and resulting in partial obstruction, seemingly coming from the duodenal muscularis mucosa. The digestive epithelium exhibited superficial necrosis, and only some duodenal glands remained. This mass exhibited coagulation necrosis affecting approximately 75% of the tissue, characterized by hyperacidophilic tissue where cellular silhouettes persisted. Within this mass, acellular, refractive, constant diameter, well-delineated spaces were observed, suggestive of the histological appearance of sutures **(Figure 4A)**. This observation is consistent with surgery during which a suture was used for hemostasis. Vascular structures, collagenous matrix, and spindle cells were identifiable, although the cell boundaries were blurred, and some nuclei were not visible **(Figure 4B)**. The spindle cell nuclei were hyperchromatic without cytonuclear abnormalities **(Figure 4C)**. The surgically resected tissue consisted exclusively of the duodenal portion.

Post-mortem histological sections of the duodenum did not reveal any lesions in the epithelium, chorion, submucosa, or duodenal muscularis, which were well preserved. There were five exophytic, pedunculated, serous lesions, 300 and 900 μm in diameter on the duodenal muscularis mucosa, consisting of adipocytes and blood capillaries, lined with activated mesothelial cells, within a moderately abundant collagenous connective tissue, with a focally myxoid appearance **(Figure 4D)**. These lesions suggested mesothelial activation due to serous inflammation, and they were observed during surgery **(Figure 2D)**. The pancreas exhibited an acute inflammatory lesion, characterized by the disappearance of part of the pancreatic acini, which were replaced by a marked fibrinous exudation, associated with numerous extravasated erythrocytes and inflammatory cells. This was indicative of acute, marked necrotichemorrhagic pancreatitis, which may be related to the signs of coelomitis seen on gross examination. Immunohistochemistry (IHC) was performed with the detection system OptiView DAB IHC Detection Kit (Roche Diagnostics, 760-700) optimized for automated IHC (Benchmark XT stainer, Ventana Medical Systems, Roche Diagnostics) using antibodies directed against SMA (Smooth Muscle Actin), Desmin, and CD117 **(Table 1)**. No positive cells were observed.

Discussion

The axolotl's clinical diagnosis was an intussusception. The underlying cause of the intussusception remained unclear, and the intraluminal mass could be necrotic intussuscepted intestine or neoplasm (spindle-cell tumor was suspected based on histopathology). Gastrointestinal disorders are common in axolotls, and surgery such as gastrotomy and enterotomy have been described.[4-5] As no description of intussusception in axolotl was available, it was assumed that the ultrasound images would be similar to those of dogs and cats. Indeed, the abnormalities in this case correlated with the appearance of intussusception described in companion animals, highlighted by the superimposed wall layers of the intussusceptum (inner bowel segment) and the intussuscipiens (outer bowel segment).[6-7]

In dogs and cats, intussusception has been associated with intestinal parasitic infestation, bacterial or viral enteritis, foreign bodies, mesenteric cysts, cecal inversion, previous abdominal surgery, nonspecific gastroenteritis, or neoplasia, and it has been documented in postparturient dogs.[8-11] Due to the diffuse nature of the lesion in the intestinal wall, the mass effect was not detected on ultrasound.

Recurrence is a common complication following surgical correction of intussusception in dogs at a location proximal to the original intussusception.[10] After correction of the intussusception, enteroplication or IRA must be performed. IRA is required in nonreducible intussusception associated with adhesions, devitalized intestine, or detection of a mass.[10,12] In the present case, IRA was chosen to remove the abnormal portion and to prevent recurrence.

The rapid deterioration of the axolotl's general condition was attributed to the coelomitis following surgery. In small animals, postoperative septic peritonitis can be associated with dehiscence of anastomotic or enterotomy sites, which has been reported to occur in 7% to 16%

of patients.[11] Anastomotic leakage was not ruled out. Coelomitis could be either primary or secondary to acute pancreatitis. In dogs and cats, acute pancreatitis has several origins that can be considered for amphibians such as toxins, hyperlipidemia, duct obstruction by complications of gastrointestinal surgery or localized peritonitis, pancreatic trauma, ischemia/reperfusion, or idiopathic.[13,14,15] Given the location of the pancreas close to the surgical site, duct obstruction or primary coelomitis may be the cause of pancreatitis. However, as both pancreatitis and coelomitis were concomitant and in the acute phase of the inflammation, the primary cause remained uncertain.

Previous case reports of neoplasia in axolotls have included cutaneous (chromatophoroma, mastocytoma, and teratoma), oral, and coelomic tumors with splenic involvement.[16-20] In our case, the observed mass originating from the duodenum muscularis mucosae presented spindle cells mixed with collagen fibers, compatible with spindle-cell tumor.[21] Differential diagnoses of intestinal tumors are leiomyoma, fibroma, neurofibroma, and gastrointestinal stromal tumor (thought to be of Cajal cell origin).[22] However, extensive necrosis prevented reaching a definitive diagnosis of neoplasia in this case. As recommended, immunohistochemistry (anti-SMA, Desmin, and CD117) was performed to refine the differential diagnosis. [21] Failure of the IHC could be related to the extensive sample necrosis or because the antibodies used were not compatible with axolotl tissue.[21]

This case describes an intussusception diagnosis and attempted treatment in an axolotl. Intussusception should be considered in amphibian patients with dysorexia and regurgitation. Ultrasonography may be a safe, useful, noninvasive diagnostic tool in axolotls to further characterize disease of the gastrointestinal tract. However, more cases are needed to draw definitive conclusions on the management of intussusception in this species.

Funding

The authors did not receive financial support for the research, authorship, and/or publication of this article.

Acknowledgments

The authors wish to thank Sophie Domingues for her assistance and language review.

REFERENCES

1) Divers SJ, Stahl SJ. Mader's reptile and amphibian medicine and surgery. 3rd ed. St. Louis (MO): Elsevier Inc.; 2019. doi: https://doi.org/10.1016/C2014-0-03734-3
2) Miller ER, Fowler ME. Fowler’s Zoo and Wild Animal Medicine. Volume 8. St. Louis (MO): Elsevier Inc.; 2015. doi: https://doi.org/10.1016/C2012-0-01362-2
3) Miller ER, Lamberski N, Calle PP. Fowler’s Zoo and Wild Animal Medicine. Volume 9. St. Louis (MO): Elsevier Inc.; 2019. doi: https://doi.org/10.1016/C2016-0-01845-4
4) Takami Y, Une Y. A retrospective study of diseases in Ambystoma mexicanum: a report of 97 cases. *J Vet Med Sci*. 2017;79(6):1068-1071. doi:10.1292/jvms.17-0066
5) Chai N. Surgery in Amphibians. *Vet Clin North Am Exot Anim Pract.* 2016;19(1):77-95. doi:10.1016/j.cvex.2015.08.004.
6) Penninck D, D’Anjou M-A. Gastrointestinal tract. In: Penninck D and D’Anjou M-A, eds: Atlas of small animal ultrasonography (2nd ed). Oxford: John Wiley & Sons; 2015, p. 259–308.
7) Neelis DA, Mattoon JS, Slovack JE, Sellon RK. Gastrointestinal tract. In: Nyland TG and Mattoon JS, eds. *Small animal diagnostic ultrasound*. 4th ed London: Elsevier; 2020, p. 481–525.

8) Lamb CR, Mantis P. Ultrasonographic features of intestinal intussusception in 10 dogs. *J Small Anim Pract*. 1998;39(9):437-441. doi:10.1111/j.1748-5827.1998.tb03752.x
9) Patsikas MN, Papazoglou LG, Papaioannou NG, Savvas I, Kazakos GM, Dessiris AK. Ultrasonographic findings of intestinal intussusception in seven cats. *J Feline Med Surg*. 2003;5(6):335-343. doi:10.1016/S1098-612X(03)00066-4
10) Larose PC, Singh A, Giuffrida MA, Hayes G, Moyer JF, Grimes JA, Runge J, Curcillo C, Thomson CB, Mayhew PD, Bernstein R, Dominic C, Mankin KT, Regier P, Case JB, Arai S, Gatineau M, Liptak JM, Bruce C. Clinical findings and outcomes of 153 dogs surgically treated for intestinal intussusceptions. *Vet Surg*. 2020;49(5):870-878. doi:10.1111/vsu.13442
11) Brown DC. Small Intestine. In: Johnston SA, Tobias KM, editors. Veterinary Surgery: Small Animal Expert. 2nd ed St Louis, Missouri: Elsevier; 2017, p. 1513-41.
12) Patsikas MN, Papazoglou LG, Paraskevas GK. Current views in the diagnosis and treatment of intestinal intussusception. *Top Companion Anim Med.* 2019;37:100360. doi:10.1016/j.tcam.2019.100360
13) Mansfield C. Acute pancreatitis in dogs: advances in understanding, diagnostics, and treatment. *Top Companion Anim Med.*. 2012:27(3):123–132. doi:10.1053/j.tcam.2012.04.003
14) Ellison GW. Complications of gastrointestinal surgery in companion animals. *Vet Clin North Am Small Anim Pract*. 2011;41(5):915-34. doi: 10.1016/j.cvsm.2011.05.006.
15) Piegols HJ, Hayes GM, Lin S, Singh A, Langlois DK, Duffy DJ. Association between biliary tree manipulation and outcome in dogs undergoing cholecystectomy for gallbladder mucocele: A multi-institutional retrospective study. *Vet Surg*. 2021:50(4):767-774. doi: 10.1111/vsu.13542.

16) Menger B, Vogt PM, Jacobsen ID, Allmeling C, Kuhbier JW, Mutschmann F, Reimers K. Resection of a large intra-abdominal tumor in the Mexican axolotl: a case report. *Vet Surg*. 2010;39(2):232-233. doi:10.1111/j.1532-950X.2009.00609.x

17) Brunst VV, Augustine LR. A spontaneous teratoma in an axolotl (*Siredon mexicanum*). *Cancer Res* 1969;29(1):223-9.

18) Khudoley VV, Eliseiv VV. Multiple melanomas in the axolotl *Ambystoma mexicanum*. *J Natl Cancer Inst* 1979;63(1):101-3.

19) Harshbarger JC, Chang SC, DeLanney LE, Rose FL, Green DE. Cutaneous mastocytomas in the neotenic caudate amphibians *Ambystoma mexicanum* (axolotl) and *Ambystoma tigrinum* (tiger salamander). *J Cancer Res Clin Oncol.* 1999;125(3-4):187-192. doi:10.1007/s004320050262

20) Modesto F, Nicolier A, Hurtrel C, Benoît J. Excisional biopsy and radiotherapy for management of an olfactory neuroblastoma in an axolotl (*Ambystoma mexicanum*). J Am Vet Med Assoc. 2021;260(4):436-441. doi:10.2460/javma.20.09.0498

21) Pellegrino V, Muscatello LV, Sarli G, Avallone G. Canine gastrointestinal spindle cell tumors efficiently diagnosed by tissue microarray-based immunohistochemistry. *Vet Pathol* 2018:55(5):678-81. doi:10.1177/0300985818777793

22) Hayes S, Yuzbasiyan-Gurkan V, Gregory-Bryson E, Kiupel M. Classification of canine nonangiogenic, nonlymphogenic, gastrointestinal sarcomas based on microscopic, immunohistochemical, and molecular characteristics. *Vet Pathol.* 2013;50(5):779-88. doi:10.1177/0300985813478211

FIGURES

Figure 1. Identification and illustration of long-axis and transverse intussusception. The inner small intestinal loop (red circle = intussusceptum) is readily identified within the outer bowel loop (white circle = intussuscipiens)

A. Long-axis view of the intussusception

B. Transverse image of the intussusception

C. Proximal view of the intussusception site

Figure 2. Surgery of the intussusception. (Cr.: Cranial; Ca.: Caudal)

A. Mass effect of intestinal loops at the beginning of the coeliotomy

B and C. Visualization of intussuscipiens (white arrow) and intussusceptum (red arrow)

D. Portion of the intestinal loops resected (between white dotted lines) with pink serosal nodules (black arrow).

Figure 3. Necropsy of the axolotl five days after the surgery. Serofibrinous coelomitis is observed.

1: Intestinal loops proximal to the IRA site

2: Site of IRA

3: Intestinal loops distal to the IRA site

4: Mesentery

5: Mesentery suture site

Figure 4. A: Histological section of the duodenum shows a multilobulated necrotic mass, protruding widely into the lumen and contributing to its obstruction (black line). Acellular,

refractive, constant diameter, well-delineated spaces are observed, suggestive of the histological appearance of sutures (arrows). (HES x4)

B: Histological examination of the duodenum showing spindle-shaped cells with blurred cell boundaries (black arrow). (HES x10)

C: Histological examination of the duodenum with details of spindle cells with hyperchromatic nuclei without cytonuclear abnormalities. (HES x40)

D: Histological examination of duodenum serosa showing exophytic, pedunculated, serous lesions of 300 and 900 µm in diameter, consisting of adipocytes and blood capillaries, lined with activated mesothelial cells, within a moderately abundant collagenous connective tissue, with a focally myxoid appearance. (HES x10)

Video 1: Movement of intestinal loops at the site of intussusception

Table 1. Immunohistochemistry performed on an intraluminal mass of the duodenum in an axolotl (Ambystoma mexicanum).

	Antigen retrieval/ enzyme	Primary antibody/ clone	Immunogen	Manufacture primary Antibody	Dilution primary antibody	Secondary antibody detection system	Chromogen/ counterstaining	Controls
SMA	CC1 cell conditioning medium, Roche Diagnostics 950-124	Monoclonal mouse anti-human muscle actin clone HHF35	SDS-extracted protein fraction of human myocardium	Dako	1/100	Mouse secondary antibody OptiView DAB IHC Detection Kit (Roche Diagnostics, 760-700)	3,3'-diaminobenzidine (OptiView DAB IHC Detection Kit (Roche Diagnostics, 760-700))	Axolotl mass: negative Healthy dog duodenum: positive
Desmin	32 min: CC1 cell conditioning medium, Roche Diagnostics 950-124	Monoclonal mouse anti-human desmin clone D33	Desmin purified from human muscle	Dako	1/400	Mouse secondary antibody OptiView DAB IHC Detection Kit (Roche Diagnostics, 760-700)	3,3'-diaminobenzidine (OptiView DAB IHC Detection Kit (Roche Diagnostics, 760-700))	Axolotl mass: negative Healthy dog duodenum: positive
CD117	32 min: CC1 cell conditioning medium, Roche Diagnostics 950-124 4 min: glutaraldehyde 2.5 µL/mL	Anti-KIT rabbit monoclonal antibody clone YR145	v-kit Hardy-Zuckerman 4 feline sarcoma viral oncogene homolog	Roche Diagnostics	1/100	Rabbit secondary antibody OptiView DAB IHC Detection Kit (Roche Diagnostics, 760-700)	3,3'-diaminobenzidine (OptiView DAB IHC Detection Kit (Roche Diagnostics, 760-700))	Axolotl mass: negative Healthy dog duodenum: positive

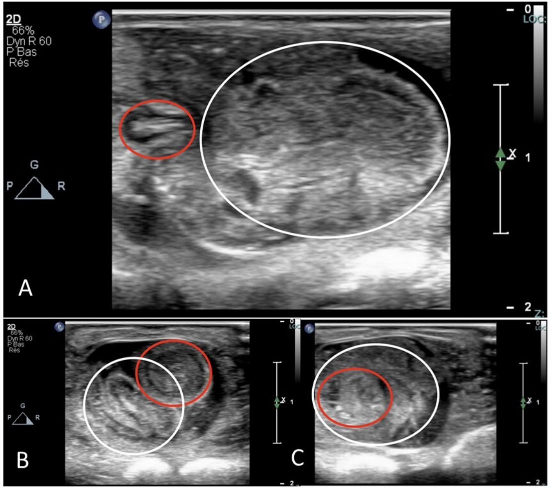
2D
66%
Dyn R 60
P Bas
Rés
G
P
R
0
1
2
A
B
C

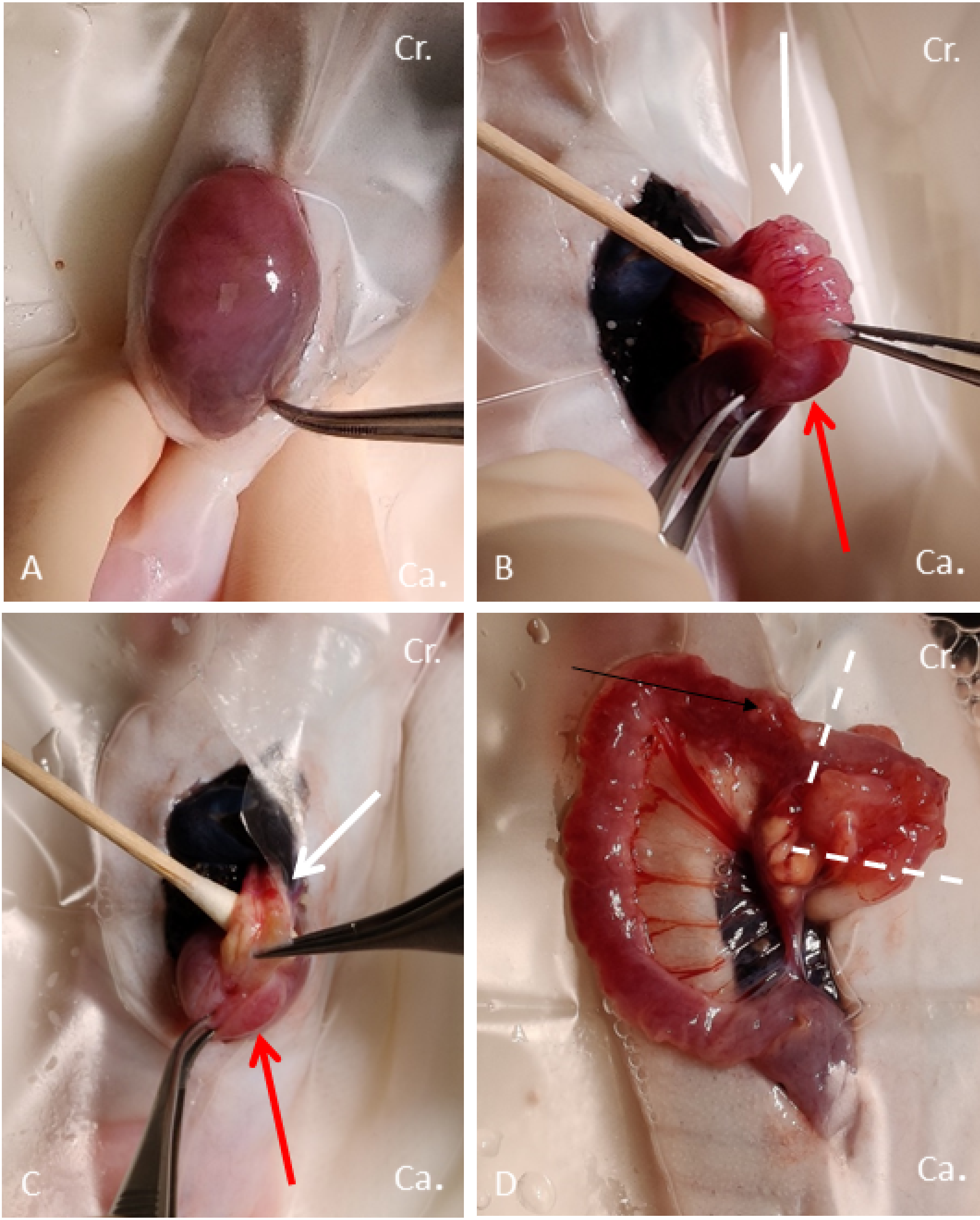
Cr.
Ca.
A
Cr.
Ca.
B
Cr.
Ca.
C
Cr.
Ca.
D

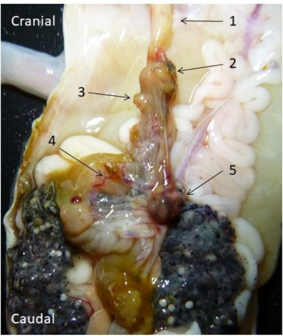

Cranial
1
2
3
4
5
Caudal

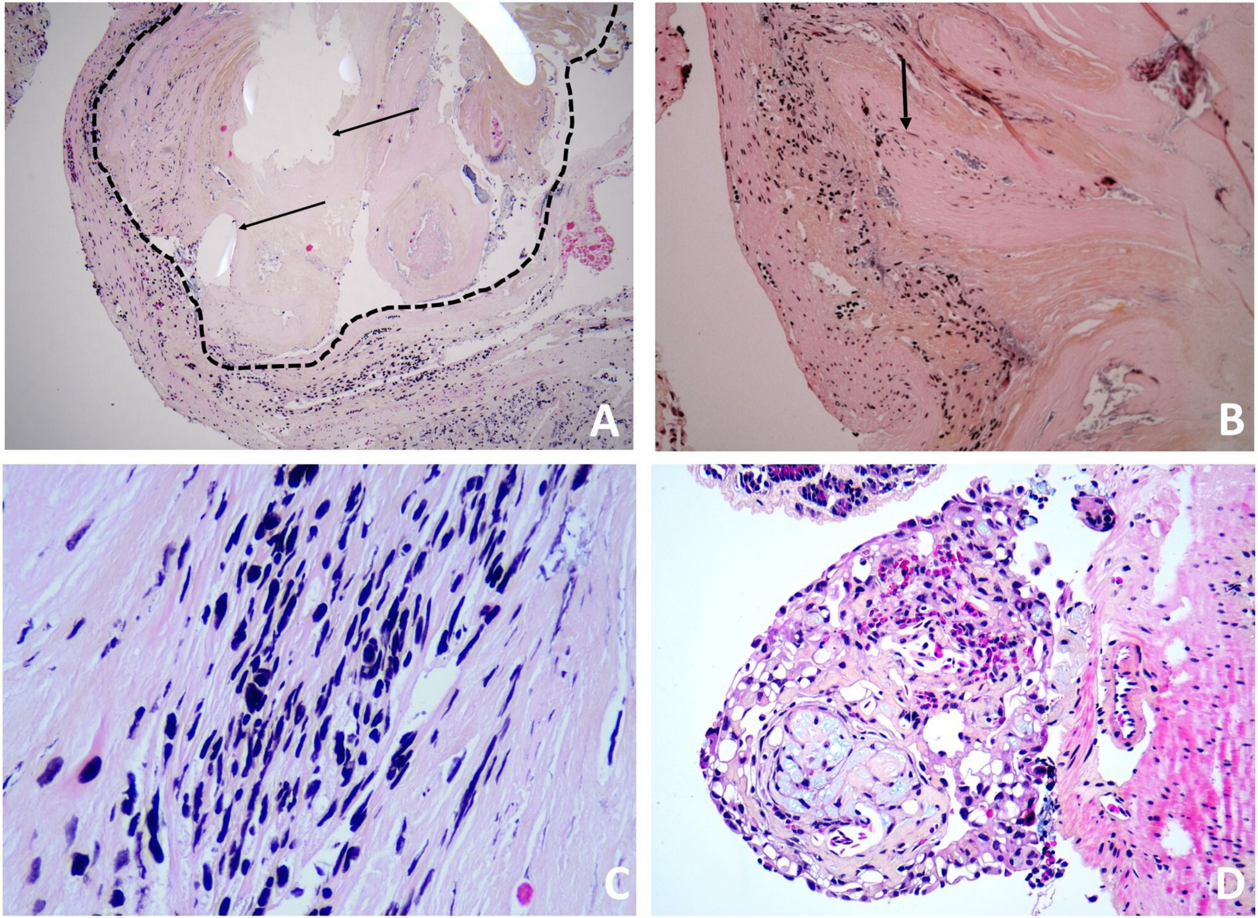
A
B
C
D